Advances in Science and Technology Research Journal

Advances in Science and Technology Research Journal 2022, 16(5), 147–154
https://doi.org/10.12913/22998624/153942
ISSN 2299-8624, License CC-BY 4.0

Received: 2022.08.08
Accepted: 2022.10.17
Published: 2022.11.01

Crystal Lattice Damage and Recovery of Rare-Earth Implanted Wide Bandgap Oxides

Mahwish Sarwar[1], Renata Ratajczak[2], Vitalii Ivanov[1], Sushma Mishra[1], Marcin Turek[3], Aleksandra Wierzbicka[1], Wojciech Woźniak[1], Elżbieta Guziewicz[1*]

[1] Institute of Physics, Polish Academy of Sciences, al. Lotnikow 32/46, 02-668 Warsaw, Poland
[2] National Centre for Nuclear Research, ul. Soltana 7, 05–400 Otwock, Poland
[3] Institute of Physics, Maria Curie-Sklodowska University, pl. Sklodowskiej 1, 20-031 Lublin, Poland
* Corresponding e-mail: guzel@ifpan.edu.pl

ABSTRACT

Rare earth (RE) elements are important for the optical tuning of wide bandgap oxides (WBO) such as β-Ga_2O_3 or ZnO, because β-Ga_2O_3:RE or ZnO:RE show narrow emission lines in the visible, ultra-violet and infra-red region. Ion implantation is an attractive method to introduce dopant into the crystal lattice with an extraordinary control of the dopant ion composition and location, but it creates the lattice damage, which may render the dopant optically inactive. In this research work, we investigate the post-implantation crystal lattice damage of two matrices of wide-bandgap oxides, β-Ga_2O_3 and ZnO, implanted with rare-earth (RE) to a fluence of 5×10^{14}, 1×10^{15} and 3×10^{15} atoms/cm^2, and post-growth annealed in Ar and O_2 atmosphere, respectively. The effect of implantation and annealing on both crystal lattices was investigated by channeling Rutherford backscattering spectrometry (RBS/C) technique. The level of crystal lattice damage caused by implantation with the same RE fluences in the case of β-Ga_2O_3 seems to be higher than in the case of ZnO. Low temperature photoluminescence was used to investigate the optical activation of RE in both matrices after performed annealing.

Keywords: wide bandgap oxides, zinc oxide, gallium oxide, rare earth, ion implantation, Rutherford backscattering spectrometry, low temperature photoluminescence.

INTRODUCTION

Wide bandgap oxides (WBO) doped with rare earths (RE) have been extensively studied because of their possible application in phosphors, lasers, plasma displays, solar cells etc. [1]. Gallium oxide is a WBO of approximately 4.9 eV bandgap and high critical electrical field strength of 8 MV/cm. The wider bandgap of β-Ga_2O_3 allows overcoming the thermal quenching effect, which is a problem in other semiconductors such as Si, ultimately enabling high temperature device operation, while large critical field allows high-voltage operation [2–5]. Due to the wide energy gap, photodetectors based on β-Ga_2O_3 are promising for solar-blind ultraviolet UV photodetectors [6]. Moreover, the high radiation hardness and chemical resistance of this material allow the devices to work even in harsh environment [7]. Zinc oxide, another WBO with a bandgap of 3.37 eV at T = 300 K [8], is a promising material for many optoelectronic and electronic applications such as solar cells, sensors, light emitting diodes and others. High quality single ZnO crystals produced on a large scale and the production of epitaxial films grown by efficient and cheaper industrial methods are additional advantages of this material. In case of luminescence, β-Ga_2O_3 emits light in the UV and visible (blue, green) region [9–11], while ZnO emits light in the violet-blue region of the spectrum [12].

Both of these WBOs are advantageous for the photonic devices working in the visible and ultraviolet spectral region, however, the spectral

emission region can be modified and enhanced by doping with a suitable dopant. Doping with RE elements can fulfill this purpose because of their characteristic sharp and narrow emission lines which may extend from infrared to ultraviolet region [13]. The origin of these emissions are the 4f intra-shell transitions, and high localization of the 4f electron shell helps to reduce the influence of the host material on RE luminescence [8]. Nevertheless, for RE in WBO, it is possible to obtain the effective resonant pumping of the f shell and thus enhancing emission spectra, which is important for applications in photonics. Because of this, both β-Ga_2O_3 and ZnO are very interesting as host materials for RE elements.

Ion implantation is an attractive method for the introduction of dopant into the host material, because of the ability to introduce any ion into the target material with control of dopant concentration by using an appropriate dose and energy in the implantation process [14–12]. Moreover, a dopant can be introduced in to the matrix of a host material with concentration higher than its solid solubility limit. There are also indications of a higher photoluminescence (PL) intensity for a material implanted with RE as compared to the one in which RE was introduced into the host material during a growth process [15]. Unfortunately, ion implantation is a destructive technique, which causes crystal lattice damage. The process of irradiation and lattice damage will be even more complex in a geometrically complicated material, such as β-Ga_2O_3, with possibility of formation of many defect complexes [16]. Moreover, most of as-implanted RE ions are optically inactive [8,17].

The crystal lattice could be recovered by using different thermal treatments at the appropriate temperature and environment. For this purpose, various types of heat treatment have been used which could also optically activate RE [17, 18]. Rapid Thermal Annealing (RTA) is one of the most effective thermal treatments which leads to RE relocation and recovery of the crystal lattice [1]. Rutherford backscattering spectrometry in channeling mode (RBS/C) is the most suitable analytical technique for RE depth profiling and studying the lattice distortion caused by radiation damage. For the evaluation of the RBS/C spectra, the SIMNRA simulation code [19] is used to find out the RE concentration from RBS random spectra and its depth profile in the crystal lattice. The Monte Carlo CHAnneling SYmulation (McChasy) code [20, 21] is used to quantify the damage depth profile from the RBS spectra in the channeling mode. McChasy simulations code has the unique ability to simulate a mixture of defects: point defects modeled as randomly displaced atoms (RDA) and extended defects as dislocations, stacking faults, and dislocation loops (DIS), which contribute to the lattice distortion. Thus, as a result of the simulation, the depth distribution for both of these types of defects is evaluated separately.

In this paper, we compare lattice damage and recovery for two WBO materials, β-Ga_2O_3 and ZnO, implanted with Eu and Sm ions and dedicated to optoelectronic applications. The structural changes caused by ion implantation and optical activation of RE after thermal annealing are carefully investigated by RBS/C and low-temperature photoluminescence (LTPL).

EXPERIMENTAL DETAILS

Commercial, single crystalline β-Ga_2O_3 substrates with the (010) orientation were provided by Kyma technologies, while ZnO epitaxial films were deposited on GaN/Al_2O_3 substrates at 300°C by Atomic Layer Deposition (ALD). Further details of epitaxial ALD processes can be found in [1].

High-resolution X-ray diffraction (HRXRD) and RBS/C measurements were performed to investigate the crystalline quality of virgin samples before implantation. The good crystalline quality of both the materials was confirmed based on the sharp and intensive XRD signals from β-Ga_2O_3 and from ZnO substrates. It should be noticed that in case of epitaxial ZnO layer, the signal was comparable to the signal coming from the GaN/Al_2O_3 substrate. Reciprocal space maps (RSMs) measured in the vicinity of chosen reciprocal lattice spots for both ZnO and β-Ga_2O_3 are shown in Figure 1 (a, b).

The χ_{min} value, as calculated from the ratio of aligned to random backscattering yield of the RBS/C spectra, was evaluated as 1.4% for single β-Ga_2O_3 crystal and as 5.3% for epitaxial ZnO/GaN films used in this experiment. Implantation with Sm and Eu ions with energy of 150 keV to fluence of 5×10^{14}, 1×10^{15} and 3×10^{15} atoms/cm^2 was performed at room temperature. The selected implantation energy allowed obtaining the 100 nm thick doped layer. This value was obtained from the McChasy simulations of the measured RBS

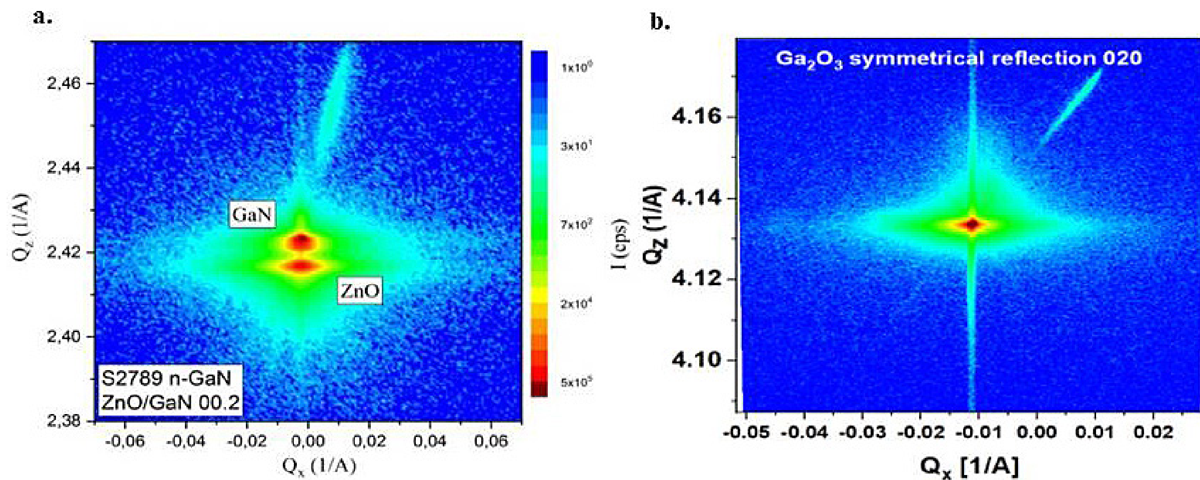

Fig. 1. Reciprocal Space Maps (RSM) of the symmetric (a) 00.2 XRD peak of ZnO, (b) 020 XRD peak of β-Ga_2O_3

spectra and is in agreement with the calculation using SRIM. Implantations were performed at the Institute of Physics, Maria Curie-Sklodowska University, Lublin, Poland, using an ion implanter equipped with arc discharge plasma ion [22]. RTA processing using an Accu Thermo AW-610 from Allwin21 Corporation system was performed at 800°C, in Ar for 0.5 min. for β-Ga_2O_3, and in O_2 for 10 min. in the case of ZnO. In this system the temperature of 800°C was achieved in 20 s, while the cooling down until room temperature was performed in a gas flow within about 300 s. The standard RBS/C measurements were performed at Helmholtz Zentrum Dresden-Rossendorf, Germany, with 1.7 MeV He- ions and using a Van de Graaff accelerator. In the RBS/C experiments, the silicon detector positioned at a scattering angle of 170° was used, with a depth resolution < 5 nm and an energy resolution < 20 keV. LTPL measurements of annealed ZnO:RE layers were performed at temperature T=5K with excitation energy E_{exc}= 3.49 eV, while the β-Ga_2O_3:RE samples were measured at T=10K with excitation energy E_{exc}= 3.53 eV. The McChasy simulations were performed based on experimental parameters obtained from the random RBS spectrum of the investigated sample as well as the aligned spectrum of the virgin sample. The detailed procedure of the McChasy simulations is described in [21].

RESULTS

RBS/C analysis

Figure 2a shows the random and <001> aligned RBS spectra of virgin ZnO and the same sample implanted with different fluence of Sm ions. The low energy part of the spectra illustrates the signal of He^{2+} ions backscattered from Zn, while the high energy part, above 1400 keV, demonstrates the signal of backscattered ions from RE. Implantation induced lattice damage can be assessed by the low energy part (left-paneled Fig. 2a) and the location of RE in the matrix is determined from the RE part of spectra (right-paneled Fig. 2a). The solid lines show the simulated spectra calculated using McChasy computer code. Figure 2b shows a comparison of implanted ZnO:Sm samples before and after annealing. As can be seen in Figure 2a, the RE signal increases with increasing fluence and, correspondingly, lattice damage is build-up, which is visible as an increase in both dechanneling and the characteristic bulk damage peak observed in the aligned RBS spectra in the 1225–1310 keV energy region. After annealing, the damage near the surface almost disappeared, but the bulk damage peak is increased, which indicates that defects might have moved towards the bulk from the surface.

Figure 2c shows the random and <010> aligned RBS spectra of virgin and implanted β-Ga_2O_3 with different fluences of Sm. In this case, the low energy part of the spectra illustrates the He^{2+} signal backscattered from Ga and the high energy part demonstrates the signal coming from RE. In the spectra of the implanted sample, a bimodal post-implanted damage profile is observed.

This kind of shape of damage peak observed in RBS/C spectra for β-Ga_2O_3 implanted with RE has already been reported [13].

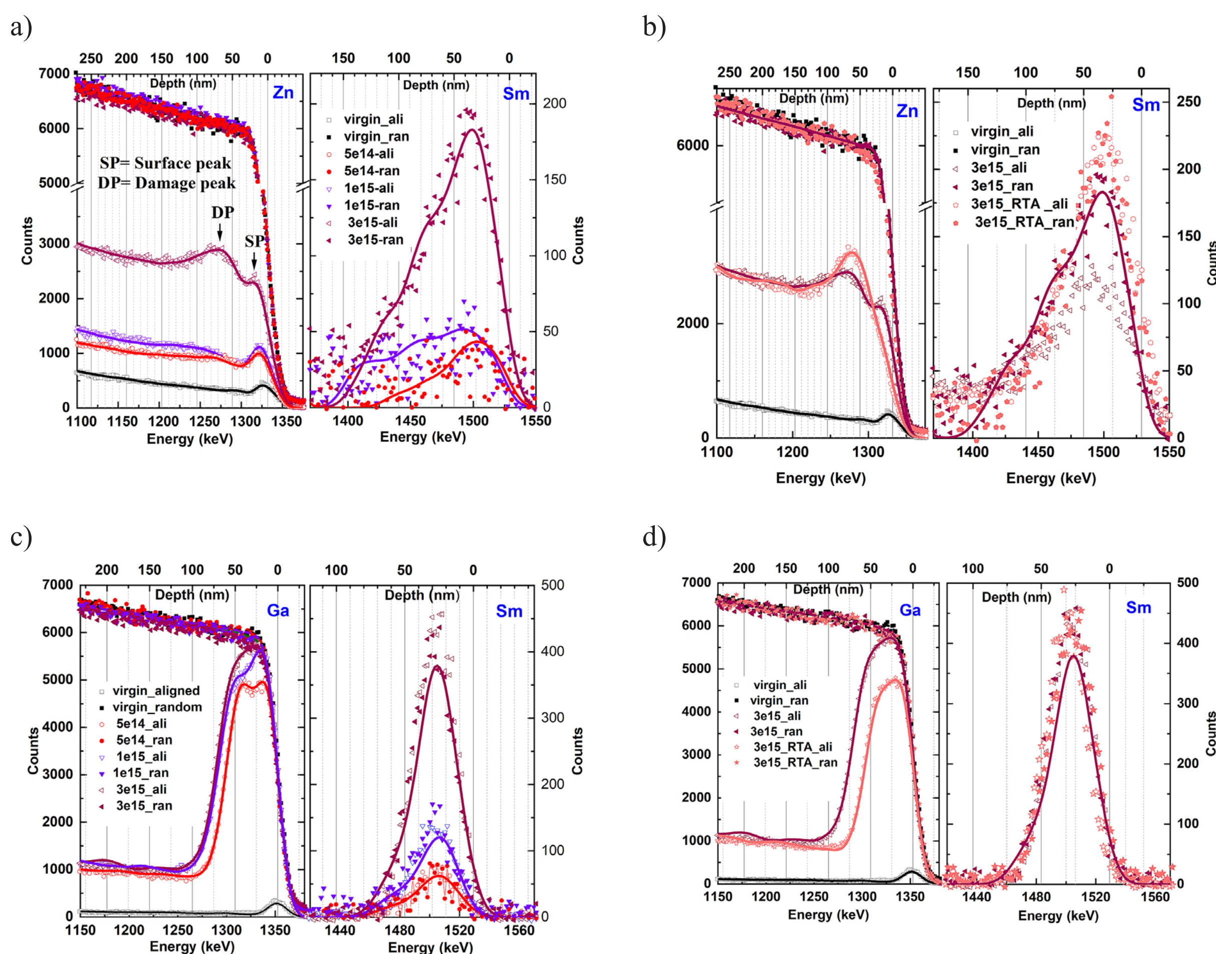

Fig. 2. Random (ran) and aligned (ali) RBS spectra for (a) ZnO implanted with Sm, (b) ZnO implanted with Sm and annealed in O_2 at 800°C for 10 min., (c) β-Ga_2O_3 implanted with Sm, and (d) β-Ga_2O_3 implanted with Sm and annealed in Ar at 800°C for 30 sec. Solid lines in all the spectra show the McChasy simulations. The discrepancies between simulated lines vs experimental points, in Zn/Ga signal energy spectral range, are less than 5%

The damage peak starts to increase with increasing RE fluence, and dechanneling level is almost similar for all fluences used, however it is higher compared to the virgin sample. Fig. 2d shows the comparison of Sm- implanted and post-implantation annealed β-Ga_2O_3 samples. Annealing leads to recovery of the lattice damage, which is evident from the decrease of the damage peak after annealing. Moreover, the defects appear to diffuse towards the surface, while the distribution of RE in the matrix remains unchanged. The calculated substitutional fraction, $\mathbf{f_s}$, i.e. the relative amount of the impurity atoms at the lattice site positions, of RE as shown in Table 1 for β-Ga_2O_3:Sm is zero for all measured fluences, both before and after annealing, indicating that the RE atoms are located in the interstitial positions. In turn, for ZnO:RE, f_s clearly shows that impurity atoms are partially located in substitutional positions after implantation, and they moved to interstitial positions only after annealing.

In order to obtain quantitative information about the damage, the McChasy simulations of the RBS/C spectra were performed. Figure 3 presents the depth distributions of RDA and DIS type of defects in ZnO:RE and β-Ga_2O_3:RE obtained as a result of the best fit of the experimental RBS/C spectra shown in Figure 2 with the McChasy code.

The McChasy simulations reveal that in both ZnO:Sm (Fig. 3a) and β-Ga_2O_3:Sm (Fig. 3b) the double damage peak occurs after implantation. For ZnO:Sm, with the fluence of 3 x 10^{15} atoms/cm^2, the atypical damage peak near the surface (called intermediate peak, IP) extends to ~25 nm, then a small depleted region and the typical bulk damage peak in the depth region from ~30nm to ~150 nm are observed. After annealing of ZnO:RE, as shown in Fig. 2b, the damage visible in the IP region has disappeared, while that observed in

Table 1. Conc. of RE calculated by SIMNRA and substitutional fraction (f_s) calculated by RBS/c spectra

Material	Nominal Conc. of RE (atoms/cm^2)	Samples name	Real Conc. of RE (10^{15}atoms/cm^2)	χ_{min} (Ga)	χ_{min} (Zn)	χ_{min} (Sm)	f_s
β-Ga_2O_3:Sm	0	Virgin	-	1.4	-	-	
	5e14	β-Ga_2O_3_Sm5e14 β-Ga_2O_3_Sm5e14_RTA	0.44 -	81.9 67.5	-	100 100	0 0
	1e15	β-Ga_2O_3_Sm1e15 β-Ga_2O_3_Sm1e15_RTA	0.96 -	89.6 78.6	-	100 100	0 0
	3e15	β-Ga_2O_3_Sm3e15 β-Ga_2O_3_Sm3e15_RTA	2.76 -	101.8 80.1	-	100 100	0 0
ZnO:Sm	Virgin	Virgin	-	-	5.3	-	-
	5e14	ZnO_Sm5e14 ZnO_Sm5e14_RTA	0.61 -	-	14.2 7.1	57 75	44 26
	1e15	ZnO_Sm1e15 ZnO_Sm1e15_RTA	1.00 -	-	14.7 11.5	61 100	40 0
	3e15	ZnO_Sm3e15 ZnO_Sm3e15_RTA	2.86 -	-	44.2 48.4	56 100	53 0

the bulk region has increased. However, the McChasy simulations reveal that the total concentration of RDA before and after annealing is similar, which clearly shows that this type of defect near the surface is not lost but diffuses towards the bulk. DIS type of defects in ZnO:Sm remains unchanged before and after annealing.

The atypical damage peak near the surface shows ~100% of RDA which extends up to ~20 nm in β-Ga_2O_3:Sm with the fluence of 3×10^{15} atoms/cm^2 (Fig. 3b). The depth damage, located close to the projected range of implanted ions, extends between 20 and 80 nm for RDA, while DIS type of defects are shifted up to ~110 nm. After annealing both concentration of RDA and DIS decrease illustrating the crystal lattice recovery. Moreover, in contrast to ZnO:RE system after annealing, the RDA defects diffuse to the surface in the case of β-Ga_2O_3:Sm.

The ZnO:Eu systems (obtained with similar fluences and energy as for ZnO:Sm) were also studied. The defect distribution for ZnO:Sm and ZnO:Eu calculated from RBS/C spectra with the McChasy code exhibits similarity, as shown in Figure 3c. This result is consistent with our previous reports [23], according to which the damage level and profile, is identical for similar masses and fluences of implanted ions. Based on that, it could be assumed that defect distributions for β-Ga_2O_3 crystals implanted with Eu and Sm should be similar.

Low-temperature photoluminescence

Typical low temperature PL spectra recorded in the visible region for both ZnO and β-Ga_2O_3 matrices implanted with Eu and subsequently annealed is shown in Fig. 4(a, b). In the inset to Fig. 4a, the sharp near-band-edge emission (NBE) peak at 375 nm and a deep-level emission (DLE) centered around 510 nm, related to native defects, can be observed for virgin ZnO. This spectrum provides the background for the Eu peak that appears in the red spectral region, close to 600 nm, for the annealed ZnO:Eu sample.

The virgin β-Ga_2O_3 crystal shows a broad emission spectrum in the visible region (Fig. 4b), where the NBE is not visible. The annealed β-Ga_2O_3:RE crystal shows the Eu peak around 625 nm indicating the optical activation of RE after annealing. However, the signal of RE in β-Ga_2O_3 is relatively weak, which means that the annealing conditions for this material need to be further optimized to enhance the Eu-related emission.

CONCLUSIONS

Rutherford Backscattering Spectrometry in the Channeling mode was used to assess the crystal lattice quality, lattice site location of RE, post-implantation damage and post-annealing recovery of the crystal structure of β-Ga_2O_3 and ZnO implanted with RE. The SIMNRA and McChasy simulations of experimental RBS/C spectra reveal that the implantation process is very different for ZnO and β-Ga_2O_3 matrices.

The implanted RE ions are situated in the interstitial positions in the β-Ga_2O_3 matrix and stay the same after annealing. In the case of ZnO, the substitutional fraction varies between

40 and 53% depending on the fluence and decreases after annealing. The McChasy simulations confirm different defect behavior in both matrices after annealing, which also suggests different mechanisms of defect creation and diffusion. For implanted to the fluence of 3×10^{15} atoms/cm^2 β-Ga_2O_3:RE, the annealing in the Ar atmosphere at 800°C for 30 s removes defects in the implanted region, while for ZnO implanted with RE with the same fluence (and similar dpa) annealed in O_2 at 800 °C for 10 mins the concentration of defect remains unchanged, the defect depth profile is only changing. According to our unpublished studies, the defects distribution in ZnO:RE is almost independent of the annealing conditions. However, it should be pointed out that the annealing atmospheres strongly influence the luminescence efficiency. In this aspect, β-Ga_2O_3:RE crystals require further investigation, because the observed luminescence response, although visible, is not very high. It is expected that the luminescence efficiency should be higher for WBO with the wider band gap, so

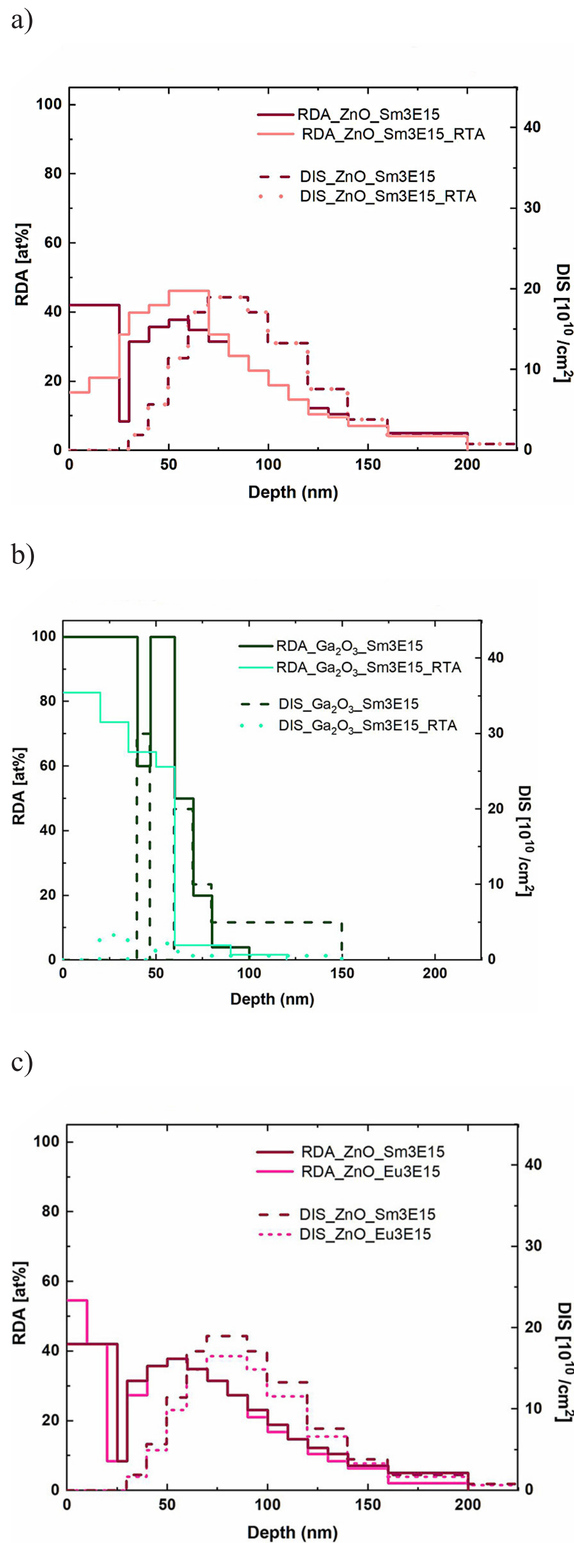

Fig. 3. Depth distributions of (a) RDA+DIS defects for implanted and annealed ZnO:Sm (b) RDA for implanted and annealed β-Ga_2O_3 :Sm + ZnO:Sm (c) RDA+DIS defects for ZnO:Eu and ZnO:Sm obtained by McChasy Simulations

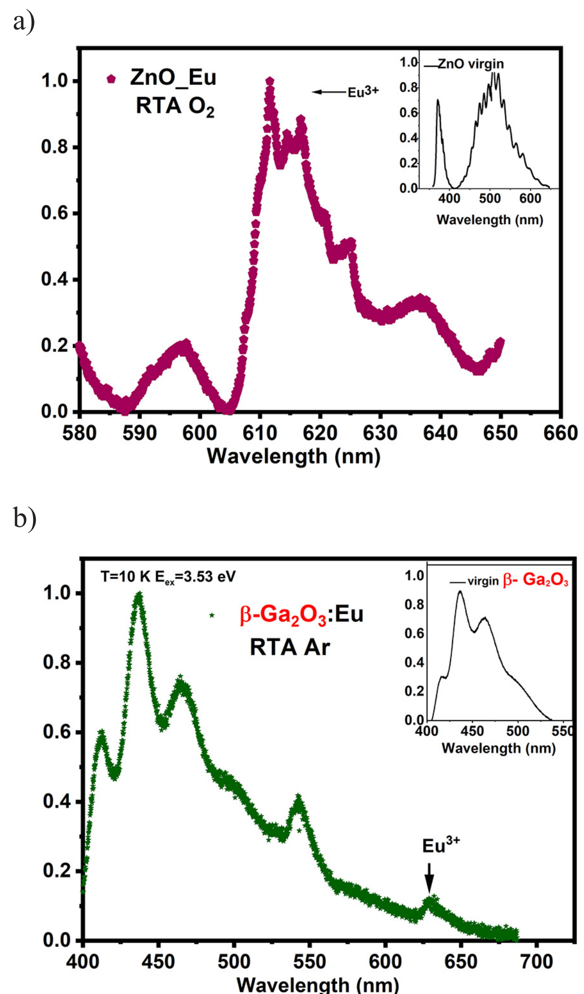

Fig. 4. LT PL spectra for (a) ZnO and ZnO:Eu annealed in O_2 at 800 °C for 10 min and (b) β-Ga_2O_3 and β-Ga_2O_3:Eu annealed in Ar at 800 °C for 30 sec

our future studies will be focused on finding the optimal annealing conditions for β-Ga_2O_3:RE.

What is interesting, contrary to widespread belief, the presented results show that the β-Ga_2O_3 matrix is less radiation resistant compared to the ZnO matrix. For β-Ga_2O_3 implanted with RE the amorphization level is reached for the fluence of 3×10^{15} atoms/cm^2 (20 dpa), while for ZnO the amorphization level cannot be achieved even after ions bombardment with the fluence up to 100 dpa. [24]

Acknowledgements

The work was supported by the international project co-financed by the funds of the Minister of Science and Higher Education in years 2021–2023; contract No. 5177/HZDR/2021/0 and Helmholtz-Zentrum Dresden-Rossendorf (20002208-ST). The publication of the paper is supported by the "Excellence in Science" program of the Polish Ministry of Education and Science (International Conference "Ion Implantation and Other Applications of Ions and Electrons", ION 2022).

REFERENCES

1. Guziewicz E., Ratajczak R., Stachowicz M., Snigurenko D., Krajewski T.A., Mieszczynski C., Mazur K., Witkowski B.S., Dluzewski P., Morawiec K., Turos A. Atomic layer deposited ZnO films implanted with Yb: The influence of Yb location on optical and electrical properties. title. Thin Solid Films. 2017; 643: 7–15.
2. Kuramata A., Koshi K., Watanabe S., Yamaoka Y., Masui T., Yamakoshi S. High-quality β-Ga_2O_3 single crystals grown by edge-defined film-fed growth. Japanese Journal of Applied Physics. 2016; 55: 1–6.
3. Stepanov S.I., Nikolaev V.I., Bougrov V.E., Romanov A.E. Gallium oxide: properties and applications- a review. Reviews on Advanced Materials Science. 2016; 44: 63–86.
4. Mastro M.A., Kuramata A., Calkins J., Kim J., Ren F., Pearton S.J. Opportunities and Future Directions for Ga_2O_3. ECS Journal of Solid State Science and Technology. 2017; 6: 356–359.
5. Wenckstern H.V. Group-III Sesquioxides: Growth, Physical Properties and Devices. Advanced Electronic Materials. 2017; 3: 1600350.
6. Armstrong A.M., Crawford M.H., Jayawardena A., Ahyi A., Dhar S. Role of self-trapped holes in the photoconductive gain of β-gallium oxide Schottky diodes. Journal of Applied Physics. 2016; 119: 103102.
7. Nikolskaya A., Okulich E., Korolev D., Stepanov A., Nikolichev D., Mikhaylov A., Tetelbaum D., Almaev A., Bolzan C.A., Buaczik A.J., Giulian R., Grande P.L., Kumar A., Kumar M., Gogova D. Ion implantation in β-Ga_2O_3: Physics and technology. Journal of Vacuum Science and Technology A. 2021; 39.
8. Ratajczak R., Mieszczynski C., Prucnal S., Krajewski T.A., Guziewicz E., Wozniak W., Kopalko K., Heller R., Akhmadaliev S. Correlations between the structural transformations and concentration quenching effect for RE-implanted ZnO systems. Applied Surface Science. 2020; 521: 146421.
9. Binet L., Gourier J. Origin of the blue luminescence of β-Ga_2O_3. Journal of Physics and Chemistry of Solids. 1998; 59: 1241.
10. Onuma T., Nakata Y., Sasaki K., Masui T., Yamaguchi T., Honda T., Kuramata A., Yamakoshi S., Higashiwaki M.J. Modeling and interpretation of UV and blue luminescence intensity in β-Ga_2O_3 by silicon and nitrogen doping. Applied Physics. 2018; 124: 075103.
11. Vasyltsiv V., Kostyk L., Tsvetkova O., Lys R., Kushlyk M., Pavlyk B., Luchechko A. Luminescence and conductivity of β-Ga_2O_3 and β-Ga_2O_3:Mg single crystals. Acta Physica Polonica A. 2022; 141: 312–318.
12. Guziewicz E., Kobyakov S., Ratajczak R., Wierzbicka A., Wozniak W., Kaminska A., Optical response of epitaxial ZnO films grown by atomic layer deposition and coimplanted with Dy and Yb. Physica Status Solidi B. 2020; 257: 1900513.
13. Lorenz K., Peres M., Felizardo M., Correia J.G., Alves L.C., Alves E., López I., Nogales E., Méndez B., Piqueras J., Barbosa M. B., Araújo J.P., Gonçalves J.N., Rodrigues J., Rino L., Monteiro T., Víllora E.G., Shimamura K. Doping of Ga_2O_3 bulk crystals and NWs by ion implantation. In: Proc. of SPIE. 2014; 8987:89870M
14. Murmu P.P., Kennedy J., Williams G.V.M., Ruck B.J., Granville S., Chong S.V. Observation of magnetism, low resistivity, and magnetoresistance in the near-surface region of Gd implanted ZnO. Applied Physics Letters. 2012; 101: 082408.
15. Hansen D.M., Zhang R., Perkins N.R., Safvi S., Zhang L., Bray K.L., Keuch T.F. Photoluminescence of Erbium-implanted GaN and in situ-doped GaN:Er. Applied Physics Letters. 1998; 72: 1244.
16. Kim J., Pearton S.J., Fares C., Yang J., Ren F., Kima S., Polyakov A.Y. Radiation damage effects in Ga_2O_3 materials and devices. Journal of Materials Chemistry C. 2019; 7: 10–24.
17. Ratajczak R., Mieszczynski C., Prucnal S., Guziewicz E., Stachowicz M., Snigurenko D., Gaca

J., Wojcik M., Böttger R., Heller R., Skorupa W., Borany J.V., Turos A. Structural and optical studies of Pr implanted ZnO films subjected to a long-time or ultra-fast thermal annealing. Thin Solid Films. 2017; 643: 24–30.

18. Alves E., Rita E., Wahl U., Correia J.G., Monteiro T., Soares J., Boemare C. Lattice site location and optical activity of Er implanted ZnO. Nuclear Instruments and Methods in Physics Research B. 2003; 206: 1047–1051.
19. Mayer M. SIMNRA User's Guide. Max Planck-Institute-fur-Plasmaphysik, Garching, Germany, 1997.
20. Nowicki L., Turos A., Ratajczak R., Stonert A., Garrido F., Modern analysis of ion channeling data by Monte Carlo simulations. Nuclear Instruments and Methods in Physics Research B. 2005; 240: 277–282.
21. Jozwik P., Nowicki L., Ratajczak R., Stonert A., Mieszczynski C., Turos A., Morawiec K., Lorenz K., Alves E. Monte Carlo simulations for ion channeling analysis of damage in dislocation-containing crystals. Journal of Applied Physics. 2019; 126: 195107.
22. Turek M., Drozdziel A., Pyszniak K., Prucnal S., Maczka D., Yushkevich Y.V., Vaganov Y.A. Plasma Sources of Ions of Solids. Instrum. Exp. Tech. 2012; 55: 469–481.
23. Ratajczak R., Guziewicz E., Prucnal S., Łuka G., Böttger R., Heller R., Mieszczynski C., Wozniak W., Turos A. Luminescence in the visible region from annealed thin ALD-ZnO films implanted with different rare earth ions. Physica Status Solidi A. 2018; 215: 1700889.
24. Lorenz K., Alves E., Wendler E., Bilani O., Wesch W., Hayes M. Damage formation and annealing at low temperatures in ion implanted ZnO. Applied Physics Letters. 2005; 87(19): 191904.